JOURNAL OF PROPULSION AND POWER
Vol. 20, No. 4, July–August 2004

Technical Notes

TECHNICAL NOTES are short manuscripts describing new developments or important results of a preliminary nature. These Notes cannot exceed 6 manuscript pages and 3 figures; a page of text may be substituted for a figure and vice versa. After informal review by the editors, they may be published within a few months of the date of receipt. Style requirements are the same as for regular contributions (see inside back cover).

High Spatial Resolution Upstream Forced Response in a Transonic Compressor

Timothy M. Hutton,* Timothy J. Leger,*
David A. Johnston,† and J. Mitchell Wolff‡
Wright State University, Dayton, Ohio 45435-0001

Nomenclature

P_{lower} = unsteady surface pressure measurement from suction side of blade
P_s = inlet static pressure
P_{upper} = unsteady surface pressure measurement from pressure side of blade
ΔP = pressure difference across the blade

Introduction

IN response to high cycle fatigue problems of modern gas-turbine engines, a considerable portion of recent research in compressor and turbine design has focused on the unsteady aerodynamic interaction of adjacent vane/blade rows. Although a fair amount of work has been performed in the prediction of the vane/blade interaction through computational fluid dynamic (CFD) models, a limited amount of experimental data exists for verification of the CFD predictions of this complicated phenomenon.

Probasco et al. compared a quasi-three-dimensional computational analysis to an experimental data set investigation compressor inlet guide vanes (IGV)–rotor interactions.[1,2] Unsteady forces on the IGV were affected by changes in axial spacing and compressor backpressure. Aerodynamic interaction, with a maximum of 62% unsteady surface pressure fluctuation, were well-modeled numerically, agreeing in phase with less agreement in the magnitude of the harmonic content. Koch et al. investigated the vortical forcing function generated by the IGV row acting on a downstream rotor.[3,4] A detailed two-dimensional mapping of the IGV wakes at three downstream axial locations showed that end wall boundary layers extending 5–10% span into the flow cause a significant decrease in the vortical forcing function in the hub and shroud regions. Three-dimensional Navier–Stokes analyses of a different transonic compressor were performed by Richman and Fleeter[5] and compared to IGV surface unsteady pressures and particle image velocimetry measurements made by Sanders et al.[6] CFD results demonstrated that interactions are highly three dimensional in nature, but tended to overpredict the steady surface pressure magnitudes whereas they underpredicted the unsteady components. This was attributed to the need for improved modeling of the viscous effects to properly simulate the interaction at the IGV trailing edge.

This study presents the acquisition of IGV unsteady surface pressure measurements at six spanwise locations, five chordwise locations, three axial spacings, and three compressor operating points at 100% design speed. The test article is a highly loaded transonic compressor system having a pressure ratio of 1.880 and an efficiency of 93.5%. The significant effects caused by variations in the compressor operating point and IGV/rotor axial spacing will be shown.

Experimental Facility

The Compressor Aero Research Laboratory (CARL) Stage Matching Investigation (SMI) facility at Wright–Patterson Air Force Base is a high-speed, highly loaded, transonic compression stage with variable speed range of 6000 to 21,500 rpm. The rig, Fig. 1, comprises a single-stage core compressor consisting of a rotor and stator with 33 and 49 airfoils, respectively, each with a 19-in. (482.6-mm) tip diameter. An IGV assembly was placed upstream of the rotor with the purpose of creating wakes consistent with those of a modern upstream stage. They have a constant solidity along the span, no net steady aerodynamic loading, and produce no turning of the flow. For these tests there are 24 vanes in the IGV row, which can be set to axial spacing of 12, 26, or 56% of the IGV chord, that is, close, mid, and far spacing, from the rotor.

A high spatial resolution, high-frequency response flexible (flex) pressure sensor array was designed and fabricated to measure the IGV surface unsteady pressures.[7] Two adjacent IGVs were instrumented each with a flex pressure sensor array to capture the unsteady surface pressures of one vane passage. The sensors were arranged in a six spanwise by five chordwise array (Fig. 2) in such a manner as to capture unsteady loading near the end walls and the trailing edge.[1,2] Calibration of the arrays for sensitivity and offset was achieved through bench tests, and a maximum uncertainty of ± 0.1 psi (0.7 kPa) was determined.[7] This value includes all errors due to random noise and temperature changes. In addition, two samples of the transducers used in the arrays were tested in the Wright State University shock tube facility and shown to have a flat response up to 30 KHz, allowing the first four harmonics of the IGV/rotor interaction in the SMI rig to be resolved.[7]

Results

Data were acquired at several axial spacings and operating points. For brevity, the ensemble-averaged response data presented are of just two periods from the 33 total available for study. The data of the pressure sensor array were processed by ensemble averaging 200 time traces to resolve the pressure difference across the IGV blade surfaces, $\Delta P = P_{\text{upper}} - P_{\text{lower}}$, as a measure of unsteady loading, and were normalized by the compressor inlet static pressure P_s (equal to the inlet total pressure). Offered is the analysis of sensor data of a common rotational speed for various throttle conditions, locations, and row spacings.

Variation with Operating Point

Figure 3 shows chordwise time traces of the differential pressure of the IGV surfaces at the 95, 50, and 5% span locations for three

Received 30 September 2002; revision received 5 April 2004; accepted for publication 16 March 2004.

*Graduate Research Assistant, Department of Mechanical and Materials Engineering. Student Member AIAA.
†Research Associate Professor, Department of Mechanical and Materials Engineering. Member AIAA.
‡Professor, Department of Mechanical and Materials Engineering. Associate Fellow AIAA.

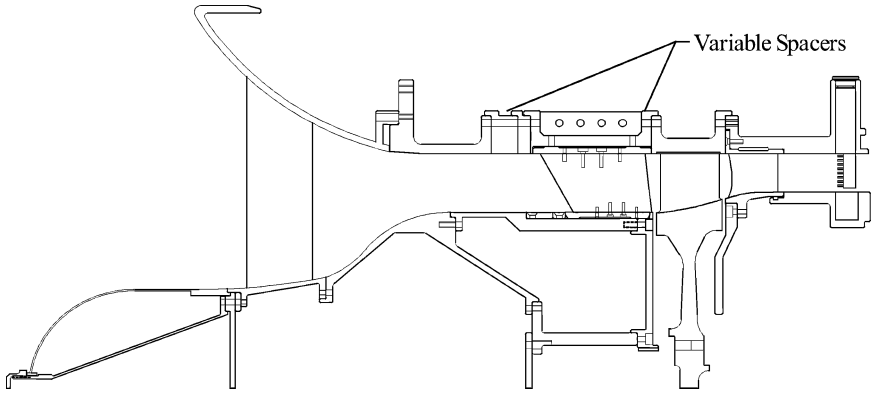

Fig. 1 Schematic of compressor rig flowpath.

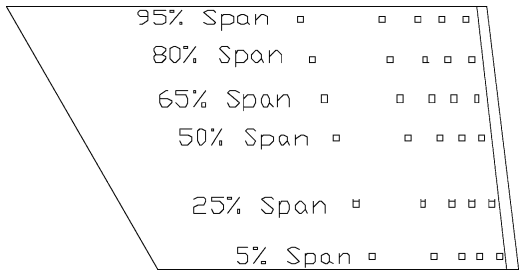

Fig. 2 Transducer locations for the IGV flex pressure sensor array.

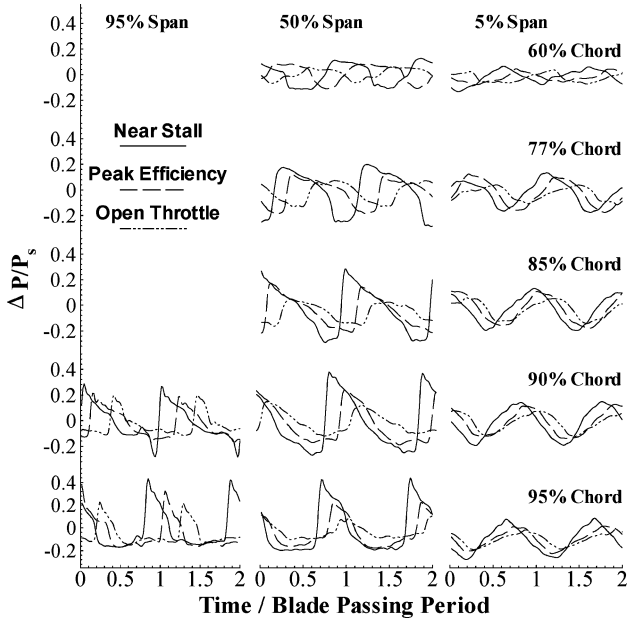

Fig. 3 Differential pressures at 95, 50, and 5% span at 100% speed and close spacing.

operating points (near-stall, peak efficiency, and fully open throttle). The time traces from top to bottom correspond to the 60, 77, 85, 90, and 95% chord locations. The peak-to-peak amplitude of the response is the highest at the 95% chord location, where it is a normalized value of 0.59, or, correspondingly, 7.9 psid (55 kPa). Evident is the response's monotonic change in amplitude and phase with compressor operating point. Moving forward from the trailing edge of the IGV shows the pressure response amplitude and rise slope decrease. At constant speed, as the mass flow rate is decreased, the rotor's oblique leading-edge shock detaches and migrates forward, forming a less oblique, stronger bow shock. This change in shock strength and impingement location is responsible for the change in amplitude and phase response with operating point. Note that the

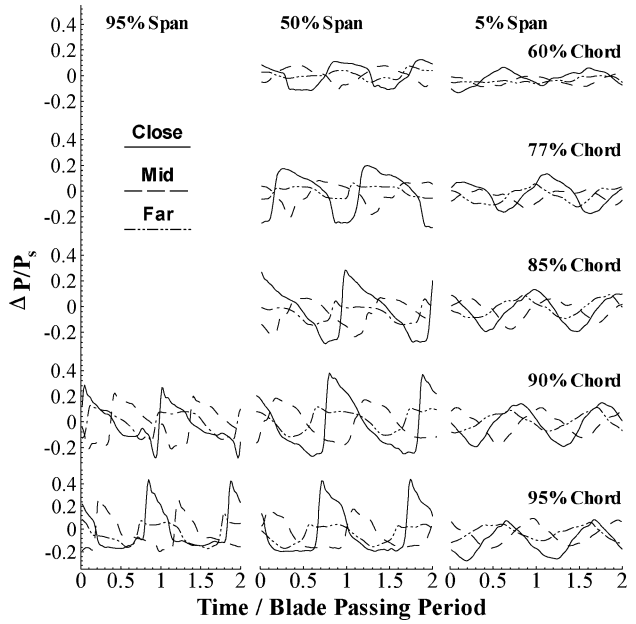

Fig. 4 Differential pressures at 95, 50, and 5% span at 100% speed and near-stall operating point.

IGV trailing edge is leaned forward, therefore, the distance between the trailing- and leading-edge of the rotor is smaller at midspan than near the hub. In addition, the chord length of the IGV increases with span. This results in a smaller bow shock interaction at higher spans for the same chord location than would normally be expected.

Variation with Row Spacing

Chordwise time traces of the differential pressure of the IGV surfaces for three spans and three axial spacings are shown in Fig. 4. The time traces from top to bottom correspond to the 60, 77, 85, 90, and 95% chord locations. Evident is an unsteady loading magnitude decrease with increased axial spacing at all spanwise locations. Also noted is the phase shift with spacing, associated with the axial component of the wave number vector of the disturbance, which varies little with spanwise location. The magnitude of the response is more sensitive to axial spacing when the forcing function originates from the supersonic relative flow region than the subsonic region. This is shown by the peak-to-peak loading decrease due to spacing at the 5% span relative to that of the 95 and 50% spans.

From a temporal Fourier analysis of the data, the left one-half of Fig. 3 presents the first four harmonics of blade passing frequency of the near stall data at 90% chord for all of the spans and axial spacings. The influence of the bow shock discontinuity and strength can be seen to contribute to the strength of the higher harmonics with increased span as the relative Mach number increases. Conversely, in the subsonic relative flow region near the hub, there is hardly

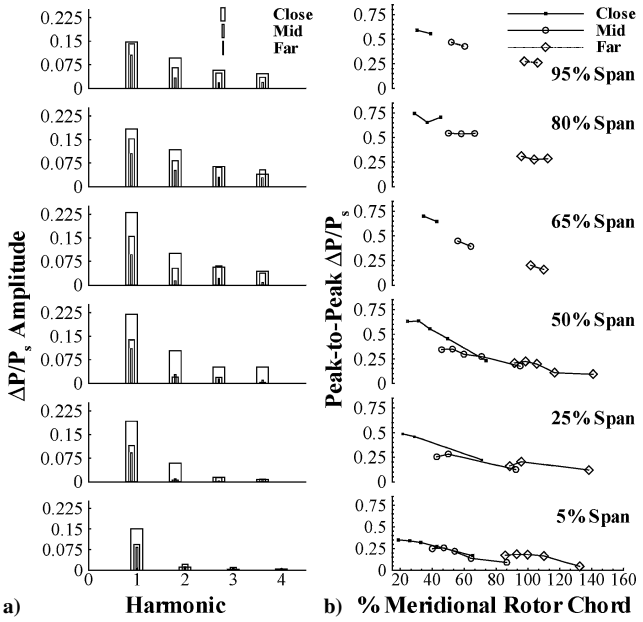

Fig. 5 Data sets of three spacings at near-stall operating point: a) frequency spectrum of differential pressure at 90% chord and b) peak-to-peak amplitudes of differential pressure.

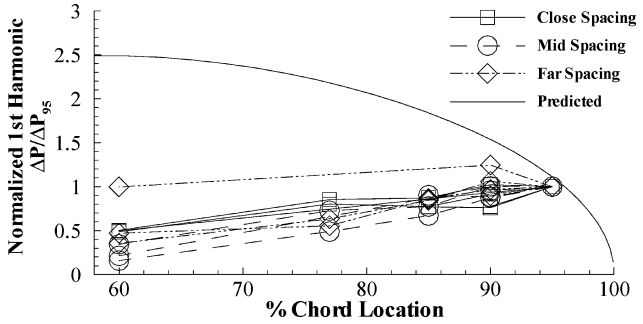

Fig. 6 Top: condensed, normalized, first harmonic differential pressure variation chord for three spacings.

any energy in the higher harmonics. The magnitudes are shown to decrease with axial spacing and to agree with the linear theory prediction that the potential field for this operating point is subresonant. The higher harmonics of the shock-induced response weaken with increased axial spacing as the expansion waves weaken the shock with distance from the rotor leading-edge locus. Depicted in Fig. 5b is the peak-to-peak amplitude of differential pressure for the three IGV spacings. The abscissa represents the distance that each sensor is located from the rotor leading-edge plane in terms of rotor chord. The curves indicate a decay of loading strength with axial distance from the rotor, which is usually monotonic; however, in some instances, there is a slight increase followed by a decrease with axial distance.

In Fig. 6, the magnitude data of Fig. 5a are normalized by that of the sensor nearest the trailing edge (95% chord) and are presented on a common ordinate scale juxtaposed against predictions from the linear theory analysis of Smith.[8] Thus, the chordwise distribution is proportional to the loading per unit forcing function magnitude. For comparison, the linear theory prediction has been normalized in the same manner as the data to yield unity differential pressure at the 95% chord location. Clearly, the linear theory analysis is conservative, overpredicting the loading magnitude, and does not predict the rearward loading distribution.

Variation with Span and Chord

The peak-to-peak amplitudes of differential pressure vs span are presented in Fig. 7 with chordwise location as the parameter. These

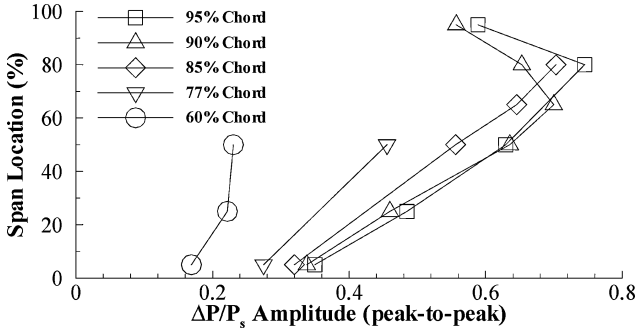

Fig. 7 Spanwise variation of peak-to-peak amplitudes of differential pressure; close spacing, near stall.

results are for the close spacing, near-stall conditions. The peak-to-peak amplitude is defined as the difference in maximum and minimum values of the time trace over one blade passing period. The amplitudes are maximum at 50 or 80% span and attenuate near the endwalls. The attenuation near the case ranges from 19 to 32% of its maximum. The end wall boundary-layer thickness extends approximately 6% of span.

Summary

Unsteady IGV surface pressures were acquired for an array of six spanwise and five chordwise locations, for a 100% speed line and three compressor operating points for three axial spacings. A significant effect was shown on the surface pressure response caused by changes in the compressor operating point and the axial row spacing for various span and chord locations. Variations in the operating point caused both a magnitude and phase change in the response with the near-stall operating point yielding the highest response. Changes in the IGV/rotor row axial spacing from 12 to 26% of the IGV chord results in a nearly 50% reduction in the magnitude of the response at midspan. At 5% span, the pressure response is less sensitive to the parametric changes controlled in this study.

Acknowledgments

U.S. Air Force Contract F33615-98-C-2895, with Technical Monitor Charles J. Cross, and the Dayton Area Graduate Studies Institute Project PR-AFIT-99-07 sponsored this research. Their support is most gratefully acknowledged. In addition, the support of the Compressor Aero Research Laboratory staff and use of the U.S. Air Force facility is gratefully acknowledged.

References

[1]Probasco, D. P., Leger, T. J., Wolff, J. M., Copenhaver, W. W., and Chriss, R., "Variations in Upstream Vane Loading with Changes in Back Pressure in a Transonic Compressor," *Journal of Turbomachinery*, Vol. 122, No. 3, 2000, pp. 433–441.

[2]Probasco, D. P., Koch, P., Wolff, J. M., Copenhaver, W. W., and Chriss, R., "Transonic Compressor Influences on Upstream Surface Pressures with Axial Spacing," *Journal of Propulsion and Power*, Vol. 17, No. 2, 2001, pp. 474–476.

[3]Koch, P. J., Moran, J., and Wolff, J. M., "3-D Inlet Guide Vane Generated Vortical Forcing Functions," *International Journal of Turbo and Jet Engines,* Vol. 17, No. 4, 2000, pp. 289–302.

[4]Koch, P. J., Wolff, J. M., and Copenhaver, W. W., "A 3-D Computational Investigation of Vortical Forcing Functions Generated by Inlet Guide Vanes," *Proceeding of the 8th International Symposium on Transport Phenomena and Dynamics of Rotating Machinery*, Vol. 1, 2000, pp. 94–101.

[5]Richman, M. S., and Fleeter, S., "Navier–Stokes Simulation IGV–Rotor–Stator Interactions in a Transonic Compressor," AIAA Paper 2000-3379, July 2000.

[6]Sanders, A. J., Papalia, J., and Fleeter, S., "A PIV Investigation of Rotor–IGV Interactions in a Transonic Axial-Flow Compressor," *Journal of Propulsion and Power*, Vol. 18, No. 5, 2002, pp. 969–977; also AIAA Paper 99-2674, June 1999.

[7]Leger, T. J., Johnston, D. A., and Wolff, J. M., "Flex Circuit Sensor Array for Surface Unsteady Pressure Measurements," *Journal of Propulsion and Power*, Vol. 20, No. 4, 2004, pp. 754–758.
[8]Smith, S. N., "Discrete Frequency Sound Generation in Axial Flow Turbomachines," Aeronautical Research Council, R&M 3709, London, 1973.

Flex Circuit Sensor Array for Surface Unsteady Pressure Measurements

T. J. Leger,* D. A. Johnston,† and J. M. Wolff‡
Wright State University, Dayton, Ohio 45435-0001

Introduction

THE acquisition of high-fidelity, high-frequency response surface pressure measurements are of interest to experimentalists in gas-turbine aeromechanical research because these data provide a means to measure indirectly the unsteady aerodynamic loading acting on an airfoil. Airfoils are typically (traditionally) instrumented from commercially available miniature pressure transducers that are flush mounted to the airfoil to prevent the transducer from aerodynamically disturbing the flow. Cavities are machined into the airfoil to accommodate the transducers, and trenches are machined to route the lead wires away from the transducer.[1–5] The main difficulty in the use of traditional transducers for high spatial resolution comes from the congestion and interference caused by the cavities and trenches required for each sensor location and the number of locations desired.

A high spatial resolution array of high-frequency pressure transducers was designed and fabricated that eliminates most of the difficulty associated with having a large concentration of transducers in a given area. Two pressure sensor arrays were applied to the suction and pressure surfaces of two inlet guide vanes (IGVs) of a transonic research compressor to measure the unsteady loading distribution induced by the passage of the bow shocks and the potential field emanating from the downstream rotor.

Flex Pressure Sensor Array

A high spatial resolution, high-frequency response flexible pressure sensor array was designed and fabricated. Two adjacent IGVs were instrumented with the flex pressure sensor array to capture the unsteady surface pressures associated with one vane passage. The sensors were arranged in a six spanwise × five chordwise array. Figure 1 illustrates the locations of the sensors. Because the effects in the end wall boundary-layer regions are of interest, transducers extend to the 5 and 95% span locations.[6] Earlier investigations indicated that the highest pressure fluctuations occur near the trailing edge of the IGV; hence, sensors were clustered near the trailing edge at the 95, 90, 85, 77, and 60% chord locations.[1]

Flexible Circuit Substrate

The flex pressure sensor array design consists of two basic components, the flexible (flex) circuit substrate and the pressure sensor dies. The flex circuit substrate serves several purposes: first, it provides the electrical connections from the sensors (dies) to the outside

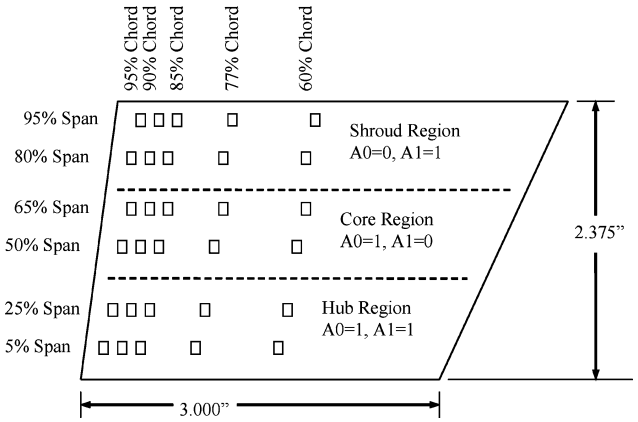

Fig. 1 Transducer locations.

of the rig in a slim, clean package, without the bundle of wires and machined trenches generally associated with instrumentation. Second, the flex circuit allows the sensor array to conform to the shape of the surface to which it is adhered. In this case, a simple shallow face 0.030 in. (0.762 mm) deep was machined into the IGV surface to compensate for the thickness of the flex substrate to allow flush mounting with the vane surface.

The flexible circuit substrate also enables the sensors to be packed to give a high spatial resolution because the wire locations for each sensor are precisely controlled. That is, individual trenches are not machined into the blade surface. Also, it provides several other significant cost benefits: First, the cost of instrumenting the blade on a per-sensor basis is decreased. The flex sensor array, including the machining and mounting, costs $42,000 or $700/sensor. The previous instrumentation by Probasco et al. cost $1250/sensor.[1] Second, the cost associated with the added complexity of connecting four individual wires for each sensor to the data acquisition system is significant when compared to utilization of the flexible circuit substrate, which only requires two connections. Although an exact dollar value cannot be calculated, the savings in terms of time and potential errors and failure modes are significant.

Two mirror-image circuit layouts were required for the suction and pressure surfaces of the adjacent vanes. A three-layer design was used: The bottom layer contains all of the traces, that is, thin film conductors, for sensor signal output. A middle layer contains all of the traces for sensor power input. The top layer contains the pads on which the sensor dies are mounted and connections to the data acquisition system are attached. To reduce the number of traces required, the negative excitation (ground) for all sensors in the array row were ganged together. Electrical connection of the flex circuit to the data acquisition system is provided by edge-board connectors with 0.050-in. (1.27 mm) spaced fingers, thereby precluding the need to solder 240 individual wires and allowing the flex circuit neck to be easily inserted through a slot in the outer casing of the rig during installation.

After the flex circuit layout was designed, it was sent to Dynamic FPC for conversion to Gerber format, a format used by printed circuit board manufacturers to apply the circuit trace masks via special plotting. The Gerber data were then sent to the Tyco Printed Circuit Group for manufacture of the flex circuit. Each layer of the design is made by first adhering a thin, 1-oz. copper film to a 0.001-in. (0.0254 mm) Kapton® sheet. The copper film is then masked and etched by the use of standard industry printed circuit board techniques. The typical size of the flex circuit traces is 0.007-in. (0.1778 mm) width with a spacing of 0.006 in. (0.1524 mm) between the traces in some areas. Small donut-shaped conductors called vias are used to connect one layer to the next. After etching, the three layers are aligned with the aid of small alignment holes and adhered together. Following this, the vias between different layers are connected by small amounts of conductive epoxy. Finally, the exposed copper pads are electroplated with 30 μ-in. (762 nm) of gold, ensuring good conductivity with the sensor dies and the

Received 30 September 2002; revision received 5 April 2004; accepted for publication 5 March 2004.

*Graduate Research Assistant, Department of Mechanical and Materials Engineering. Student Member AIAA.
†Research Associate Professor, Department of Mechanical and Materials Engineering. Member AIAA.
‡Professor, Department of Mechanical and Materials Engineering. Associate Fellow AIAA.